



This is a repository copy of *Rubber friction and the effect of shape*.

White Rose Research Online URL for this paper:
<http://eprints.whiterose.ac.uk/150426/>

Version: Accepted Version

Article:

Hale, J., Lewis, R. orcid.org/0000-0002-4300-0540 and Carré, M.J. (2020) Rubber friction and the effect of shape. *Tribology International*, 141. ISSN 0301-679X

<https://doi.org/10.1016/j.triboint.2019.105911>

Article available under the terms of the CC-BY-NC-ND licence
(<https://creativecommons.org/licenses/by-nc-nd/4.0/>).

Reuse

This article is distributed under the terms of the Creative Commons Attribution-NonCommercial-NoDerivs (CC BY-NC-ND) licence. This licence only allows you to download this work and share it with others as long as you credit the authors, but you can't change the article in any way or use it commercially. More information and the full terms of the licence here: <https://creativecommons.org/licenses/>

Takedown

If you consider content in White Rose Research Online to be in breach of UK law, please notify us by emailing eprints@whiterose.ac.uk including the URL of the record and the reason for the withdrawal request.



eprints@whiterose.ac.uk
<https://eprints.whiterose.ac.uk/>

Rubber Friction and the Effect of Shape

John Hale*, Roger Lewis, Matt J Carré

Email: jhale1@sheffield.ac.uk

Department of Mechanical Engineering, University of Sheffield, Mappin Street, Sheffield S1 3JD, UK

Abstract

Contrary to the classic laws of friction, rubber friction is not independent of shape. The friction of three shapes of the same rubber compound sliding over a dry-rough surface was measured. The three shapes had the same nominal contact area but different sliding direction-lengths and widths. Frictional differences were found between all three shapes at sliding speeds of 10 mm/s and 0.5 mm/s. The effect of frictional heating and other friction mechanisms that cause these differences are evaluated and discussed.

Keywords: Elastomer, Friction, Wear, Sliding

1. Introduction

Understanding the dry frictional performance of rubber has implications to mechanical efficiency and more importantly, personal safety e.g. footwear and automobile tyres. Amontons' friction law states that the shape of a body that is sliding on a dry surface will have no effect on the coefficient of friction (μ). However, rubber does not obey this law [1]. The analytical theories used to predict the dynamic friction (μ_k) of rubber sliding over dry rough surfaces, by Persson [2] and Heinrich and Klüppel [3] do not include parameters to account for changes in a rubber blocks' height or shape. These theories predict rubber friction using the rubber's viscoelastic properties, the contacting surface's multiscale roughness, the contact pressure and slide velocity. However, studies conducted to determine the μ between rubber and rough surfaces find significant differences to occur with dissimilar rubber tread patterns of the same material in the same slide conditions. This has been found for both tyre-road and shoe-surface experiments [4,5]. Although frictional differences are found with different treads, very little scientific rationale is provided to explain why. This is partly because the treads used are too complicated in geometry to determine any clear influencing factors. A study testing the μ_k of a rubber block orientated in two ways found the sliding direction-length of the shape to have a frictional effect, with the longer shape (Figure 1) producing lower μ_k due to increased frictional heating [1] which often reduces friction via elastic softening of the rubber [6].

It is implied that sliding at slow velocities ($v < 1$ mm/s) would find no differences for rubber shape as little frictional heat is generated and is quickly dissipated, not influencing friction.

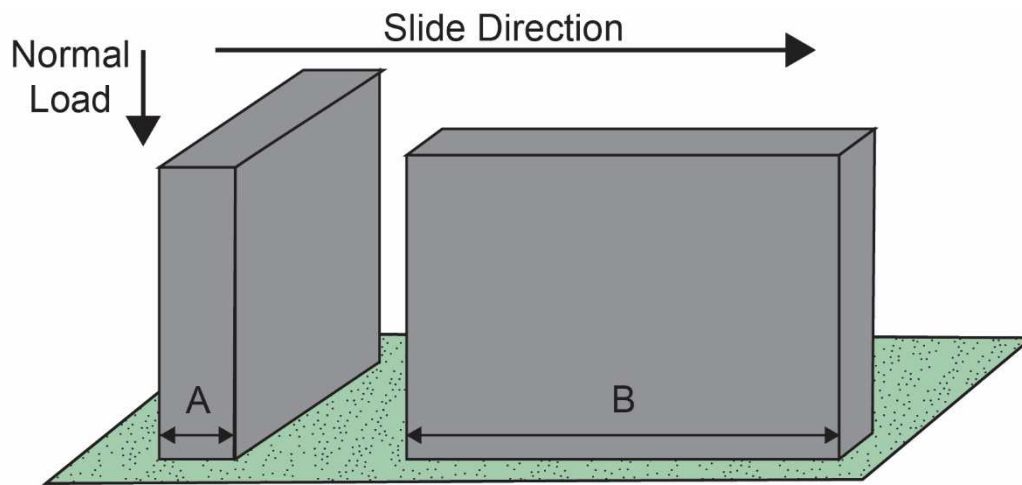


Figure 1. Two rubber blocks of the same shape orientated differently in respect to the slide direction. A and B refer to the two different slide-direction lengths. Theory suggests that B will produce lower μ_k due to increased frictional heating.

It has also been proposed that rubber's hysteric contribution to friction can be subcategorised into "surface" and "bulk" hysteresis [7], thus implying that tread of a greater height will demonstrate higher μ due to an increased "bulk" hysteresis through a reduction in the tread stiffness. This is directly opposed by the findings of Maegawa et al. [8] which states that the taller the tread element, the greater the presence of friction-induced torque which reduces the total real contact area, leading to a decreased friction force. This discrepancy in the literature could be due to the different counter surfaces used in both studies. Maegawa et al. [8] used a smooth poly(methyl methacrylate) (PMMA) surface and Kummer [7] used rough road surfaces. The friction mechanisms present when sliding rubber over rough and smooth surfaces can greatly differ in both nature and magnitude. For smooth surfaces, the stress concentration that typically forms at the leading edge of sliding viscoelastic materials [9,10], is less likely to significantly affect the wearing of the rubber. Therefore, the contact area of a rubber block with lower stiffness is smaller, resulting in lower friction coefficients [8]. Surface roughness also alters the presence of adhesion which is thought to reduce as roughness is increased [11]. As shown, many studies indicate that rubber tread shape and height influence the friction of rubber. However, uncertainties are still present as to exactly how they have an effect, especially on rough, dry surfaces.

Within this study, sliding experiments were performed on three different shaped blocks of rubber, clamped at different heights, to identify the influencing factors of rubber tread that may cause frictional differences when rubber slides on rough surfaces.

It is hypothesised that at sliding velocities above 1 mm/s, shape will have a frictional effect, with the longest sliding-direction shape having the lowest friction due to increased frictional heating. At velocities below 1 mm/s, due to frictional heating being negligible, frictional differences between shapes are not expected. Additionally, it is theorised that higher friction will be observed for an increase in tread height due to increased bulk hysteresis.

2. Methodology

2.1 Surface Characterisation

A single rough surface ($R_a = 72 \mu m$, $R_q = 91 \mu m$) was used in all sliding experiments. The surface was constructed of a 20 mm thick plywood base, topped with a sand-acrylic paint mix to give an isotropic rough texture. This type of surface is used in sports such as tennis and in areas where high friction is desired e.g. sides of roads and on pedestrian stairways.

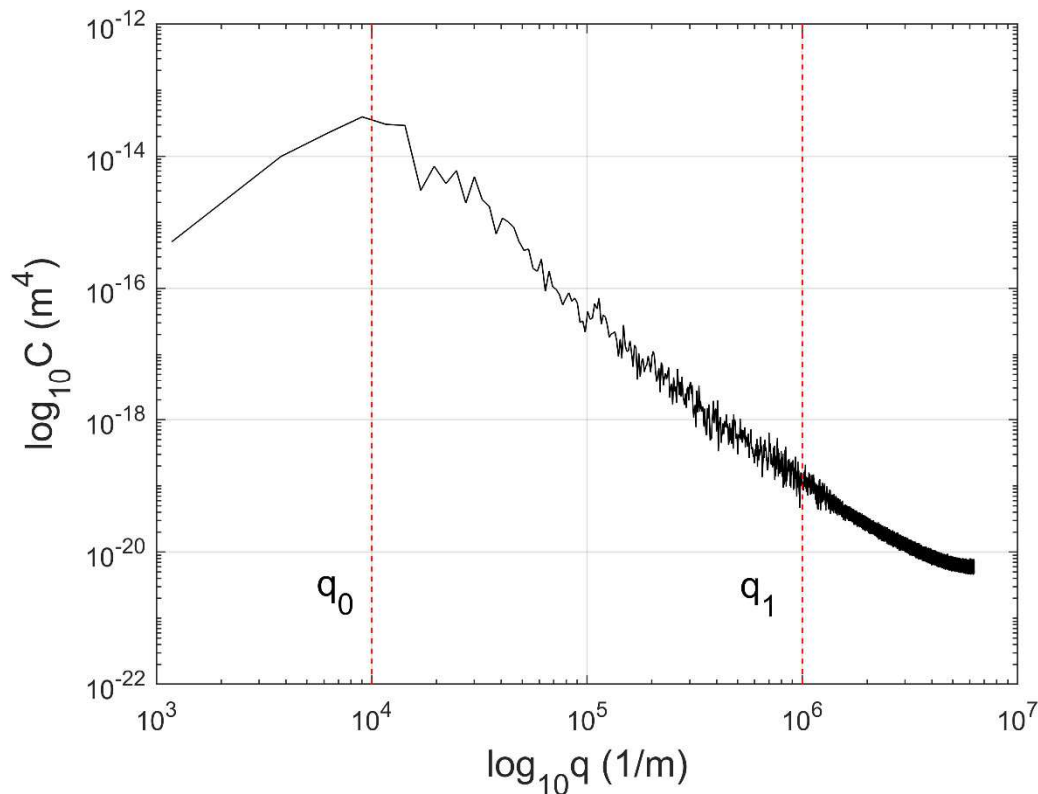


Figure 2. Power Spectral Density (PSD) graph for the rough surface. q_0 and q_1 represent the range of wavevectors on the surface's topography.

To characterise this surface, a Power Spectral Density (PSD) was obtained (Figure 2). This was achieved using non-contact profilometry (Alicona InfiniteFocus SL, Optimax, Leicestershire, UK). The PSD of a surface details the wavelengths across multiple decades that are characteristic of the measured topography. Figure 2 shows that the surface has

roughness wavelengths ranging between $q_0 \approx 0.5$ mm (which corresponds to the fine sand particle size, that gives the surface its macro texture) to $q_1 \approx 0.2$ μm (which relates to the size of dust particles and other contaminants on the surface that will provide the surface with its smallest wavelengths of roughness). For more details regarding PSDs as a surface measure, see Persson et. al [12].

2.2 Rubber Characterisation

All rubber treads used were cut from a sheet of commercially available Styrene Butadiene Rubber (SBR) (purchased from Rubberstock.com) and had a Shore A hardness value of 75. This rubber has applications in automotive and footwear industries.

To characterise this rubber, as shown in Figure 3, a viscoelastic master curve was generated which details the real (storage) and imaginary (loss) modulus of the rubber over 20 decades of frequency. To generate these curves, Dynamic Mechanical Analysis (DMA) was used, utilising the time-temperature superposition principle (DMA VA2000, Metravib, France). Testing was conducted on a sample of SBR between 1 and 30 Hz at several temperatures between -50 and 100°C with a reference temperature of 26°C. The dynamic strain was set at 1×10^{-3} %.

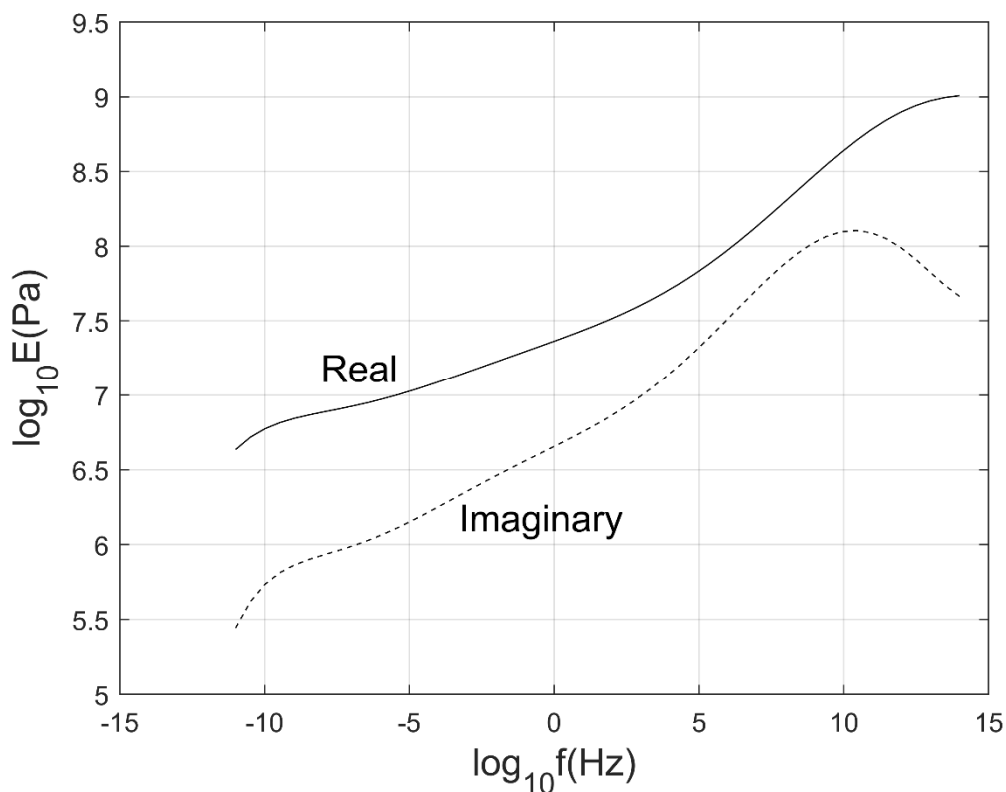


Figure 3. Real and Imaginary modulus master curves for an SBR rubber.

The loss modulus of a rubber informs as to the internal energy loss that occurs when the rubber is oscillated at a range of frequencies / temperatures, hence the hysteric response. Figure 3 shows that, up to 1×10^{10} Hz, an increase in frequency, which could be caused by an increase in slide velocity, leads to greater internal energy loss. In turn there is a greater hysteric and, potentially, frictional effect. However, as is shown, if these frequencies increase further, the hysteresis contribution to friction will peak before reducing. Furthermore, the modulus of rubber exhibits a relationship with temperature which is the inverse of the frequency relationship. Hence, although an increase in slide velocity would generate higher oscillating frequencies in the rubber and therefore greater hysteresis, the frictional heating caused by the increase in slide velocity will bring down the hysteric energy loss. The way in which these two mechanisms counter one another underpins the dry frictional performance of sliding rubber.

When analysing wet-surface sliding friction, the rubber's surface roughness has been shown to be influential [13]. On the contrary, the surface roughness of rubber has been shown to have little effect on the friction of rubber on dry rough surfaces [14], unless the rubber has been sufficiently run-in, which can cause sliding friction inversion symmetry [15]. As the rubber tread samples are tested without run-in and on a dry rough surface, rubber surface roughness measures were not taken.

2.3 Experimental Procedure

A Universal Mechanical Tester (UMT) tribometer (CETR-UMT2, Bruker, Massachusetts, USA) was used to slide the rough surface beneath three rubber samples of different geometries at 0.5 mm/s and 10 mm/s. Unlike at 10 mm/s, at 0.5 mm/s it is predicted that frictional heat will be negligible [16]. This allows us to compare how frictional heat influences μ_k . All samples were loaded with a nominal contact pressure of 0.1 MPa, produced by applying a normal load of 10 N. The UMT control system maintained this normal load throughout sliding. Slides were 30 mm in length. Three to five slides were performed for each rubber shape in each condition. After each slide, the rubber and surface were lightly brushed with a fine-bristled paint brush to remove the potential influence of wear contamination at the rubber-surface interface. The experimental set-up is shown in Figure 4.

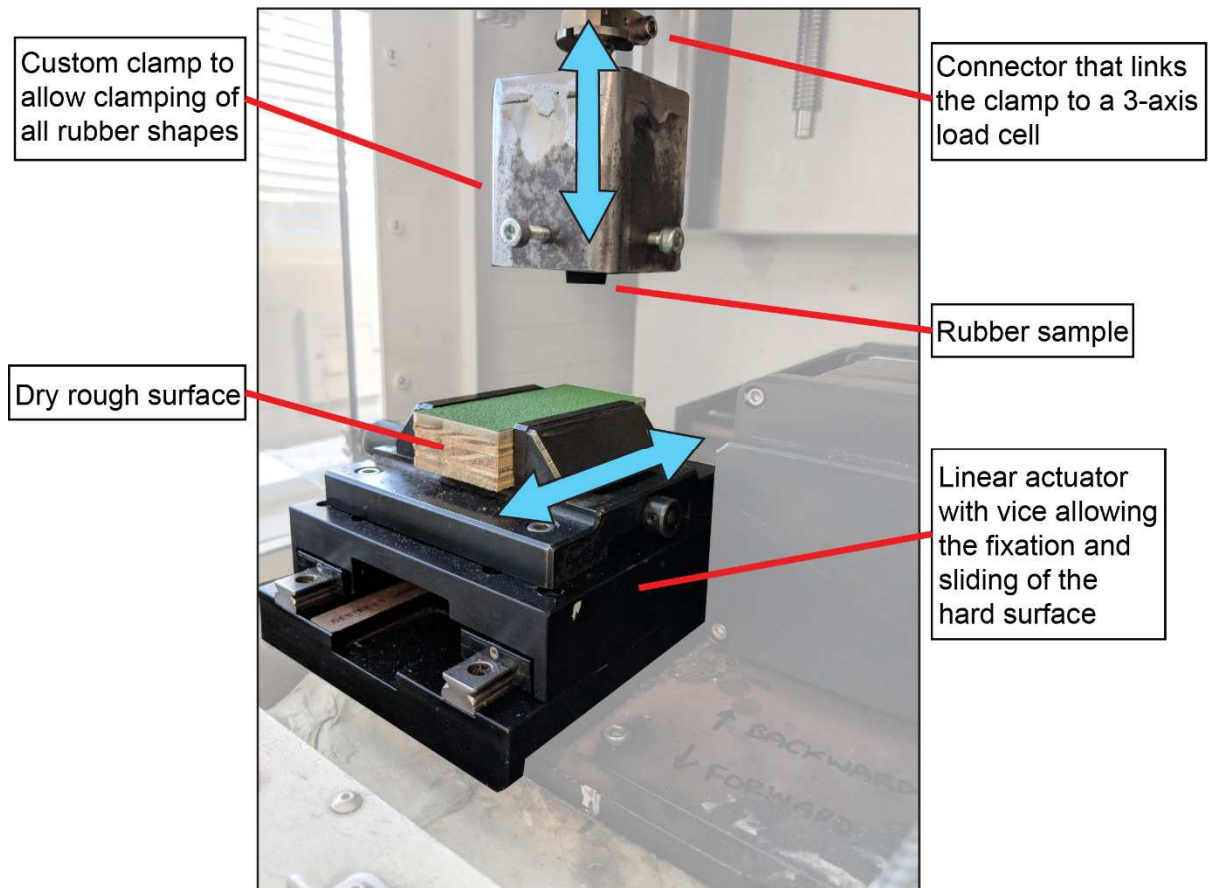


Figure 4. Experimental set-up.

Figure 5 details the three shapes of rubber tread used during this study (S1, S2 and S3). All samples had an equal nominal contacting surface area (100 mm^2) but, considering the rubber treads as end-loaded cantilever beams, differed in second moment of area (I_{xx}) in the slide direction (x). This ensures the frictional differences observed in some studies as a result of differing nominal contact area [17] were accounted for.

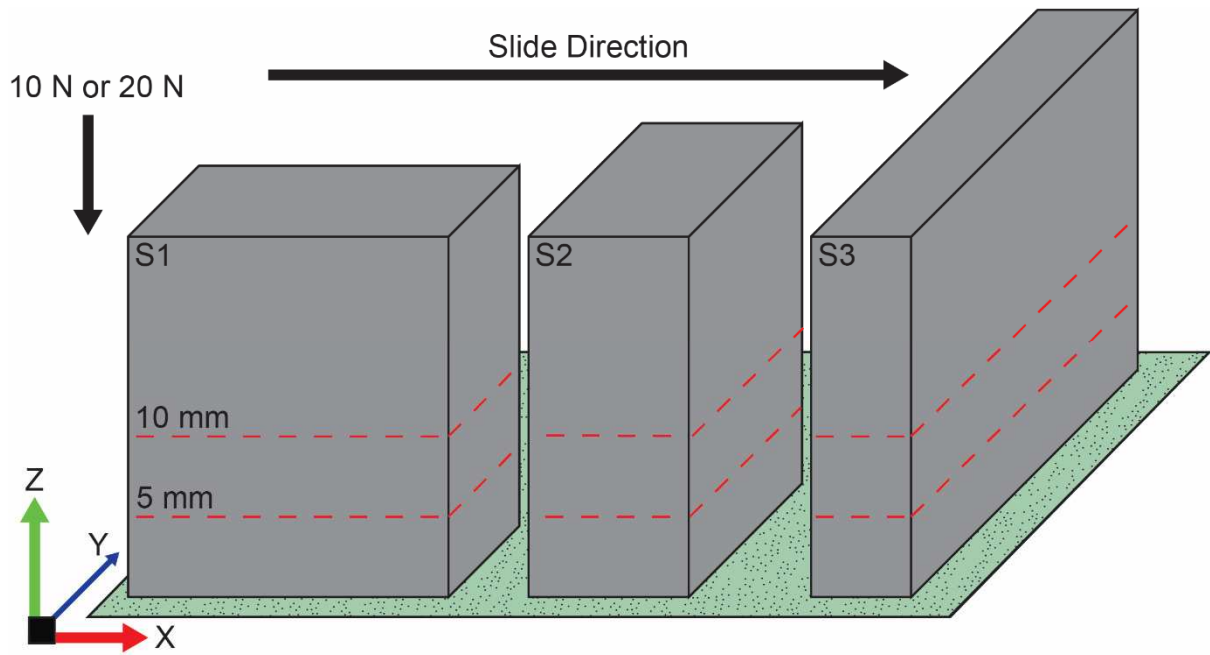


Figure 5. All shapes of rubber tested at clamp heights of 5 and 10 mm.

Using Equation 1, the I_{xx} values were calculated as 3333 mm^4 , 833 mm^4 and 208 mm^4 for treads S1, S2 and S3 respectively.

$$I_{xx} = bh^3/12$$

Equation 1

where 'b' is the base width in y , and 'h' is the base length in x . Tread height was modified by clamping the rubber tread elements at two different points along their height (5 mm and 10 mm in the z -axis from the contacting face). Equation 2 was used to determine the beam stiffness (K) of the rubber during each test. Beam stiffness here refers to the stiffness of the rubber tread element, not to be confused with the modulus 'E', which represents the tensile modulus material characteristic.

$$K = 3EI_{xx}/l^3$$

Equation 2

In Equation 2, the tread clamp height was used for l and the tensile modulus of 3 MPa was used for E .

2.4 Wear Analysis

For one series of tests (0.1 MPa, 0.05 mm/s and 5 mm tread height), all three rubber samples had their mass measured (Satorius BasicPlus BP210D, Göttingen, Germany) before and after three slides. Additionally, to investigate the wearing regions on the rubber, three slides were

performed at higher pressure (0.2 MPa) and at a 10 mm/s slide velocity, clamped at 5mm. Photos were taken before and after these slides.

2.5 Definition of μ_s and μ_k

μ_s is defined as the μ that is overcome to initiate sliding and μ_k is the μ needed to be overcome to maintain motion. Figure 6 is a μ -time trace labelled with μ_s , which is taken as a single value and μ_k which is the average of the proceeding readings as sliding is maintained.

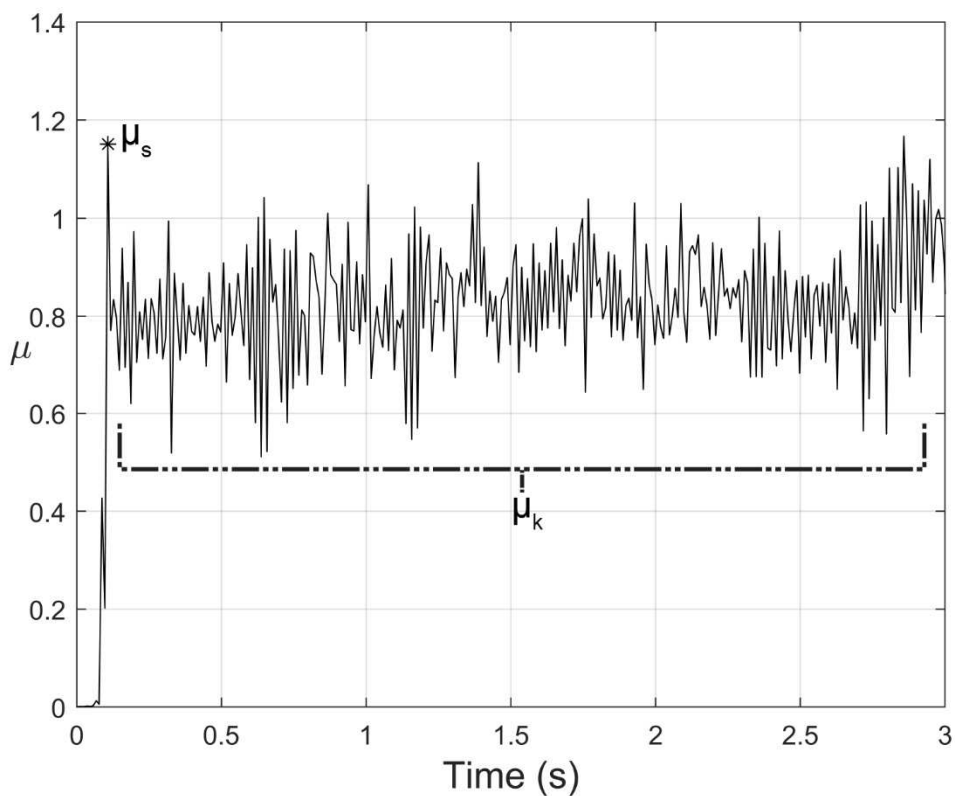


Figure 6. An example μ -time trace with annotated with the static (μ_s) and dynamic (μ_k) friction coefficient. μ_k is calculated as the average of all μ values that follow the μ_s value.

2.6 Data Analysis

Two univariate between groups one-way analysis of variance tests (ANOVA) were conducted. These investigated the effect of slide velocity, tread height and shape length, as well as their consequent interactions on both μ_s and μ_k . Bonferroni post hoc tests were performed to investigate the effects of all three individual shape lengths while controlling Type 1 error [18]. Prior to the running of this analysis, normality checks were performed. All statistical analysis was conducted using IBM SPSS Statistics 25.

3. Results

Figure 7 and 8 show that beam stiffness of the tread element had no significant effect on μ_s and very little effect on μ_k . Although, there is a slight negative correlation between beam stiffness and μ_k it is not strong enough to conclude that increasing tread stiffness decreases μ_k . Similar trends are shown between μ_k and beam stiffness at both velocities, but at lower magnitudes of μ_k during sliding at 0.5 mm/s.

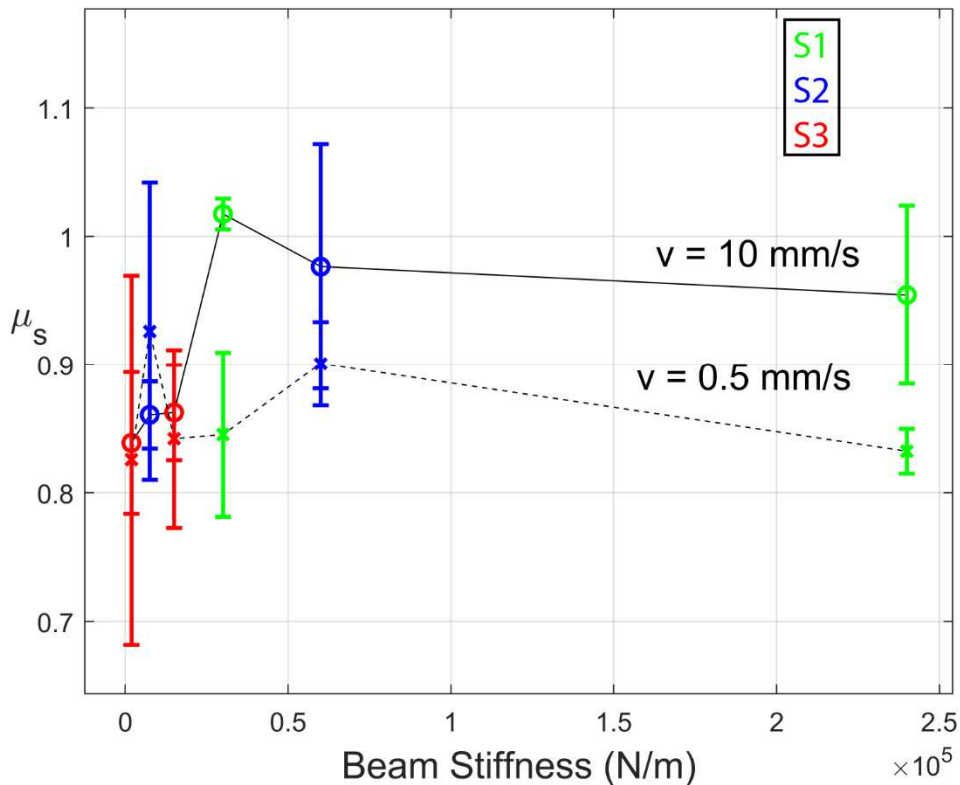


Figure 7. μ_s against beam stiffness for all shapes at both 5 mm and 10 mm tread height at 0.1 MPa. Dotted line indicates $v = 0.5$ mm/s and solid indicates $v = 10$ mm/s. Error bars represent the standard deviations in μ_s over the three tests of each condition.

No significant difference is found in μ_s with change in tread height or shape length. Significant difference in μ_s is only found for the change in velocity ($F(1,57) = 12.517, p = 0.001$). Here, the increase in velocity from 0.05 mm/s to 10 mm/s resulted in an increase of mean μ_s from 0.86 to 0.95.

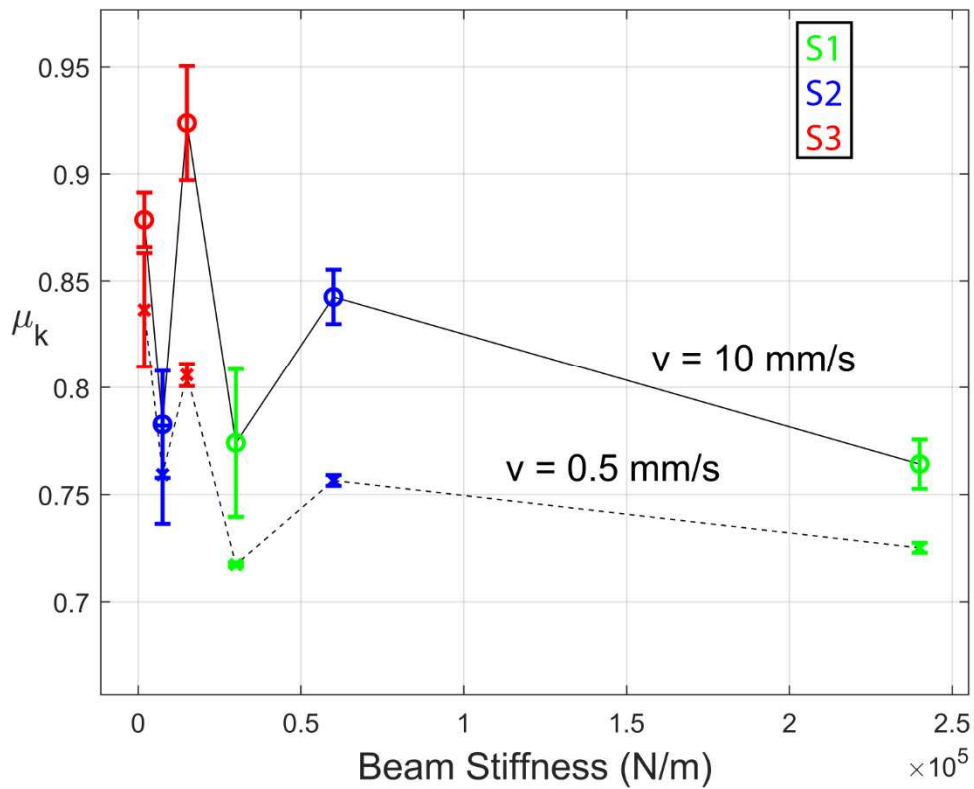


Figure 8. μ_k against beam stiffness for all shapes at both 5 mm and 10 mm tread height at 0.1 MPa. Dotted line indicates $v = 0.5$ mm/s and solid indicates $v = 10$ mm/s. Error bars represent the standard deviations in μ_k over the three tests of each condition.

No significant difference in μ_k for different tread height was recorded. However, very strong significance was obtained for the change in μ_k that occurred for the change in slide velocity ($F(1,57) = 18.588, p < 0.001$) and shape length ($F(2,56) = 30.654, p < 0.001$). Additionally, Bonferroni post hoc tests found significant difference between all shape length subgroups ($p < 0.05$ for all group comparisons). As shown in Figure 9, mean μ_k values increased with slide velocity, rising from 0.77 at 0.5 mm/s to 0.83 at 10 mm/s. μ_k and shape length produced a negative correlation.

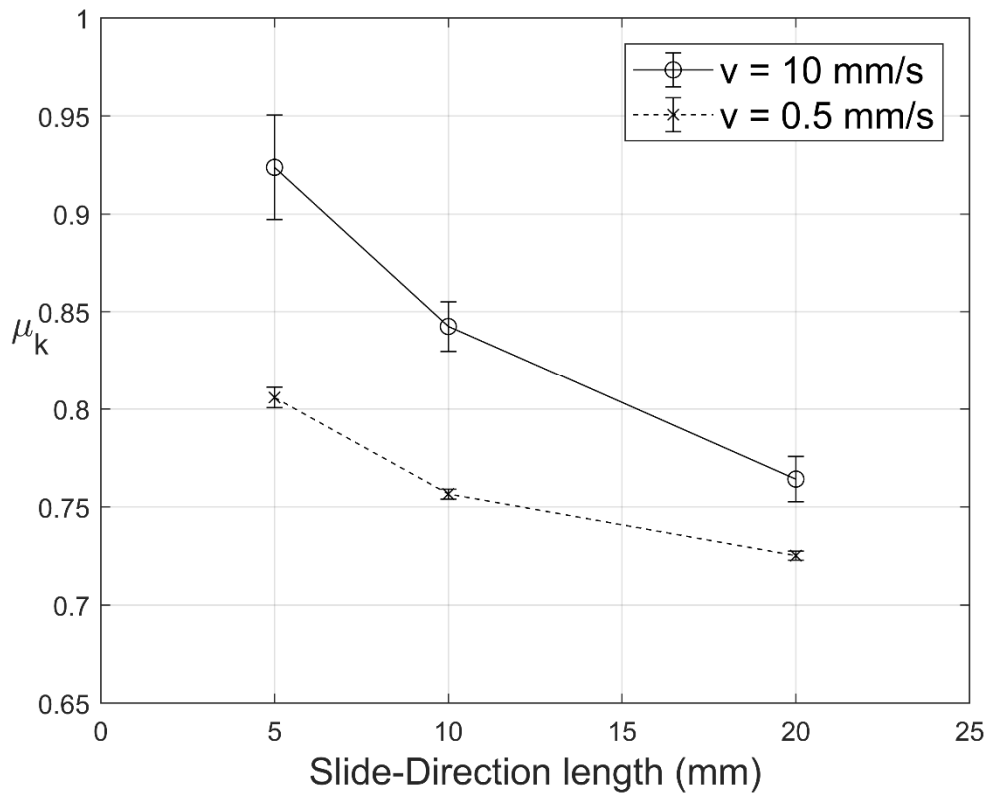


Figure 9. The relationship between μ_k and the shape's slide-direction length. For each shape the increased velocity increases μ_k .

When sliding with a pressure of 0.1 MPa and at a velocity of 0.5 mm/s, different amounts of wear were measured. Figure 10 shows that S1 wore the least, with a mass loss of 1.44 mg, followed by S2 with a mass loss of 1.72 mg. S3 recorded the greatest mass loss of 4.10 mg.

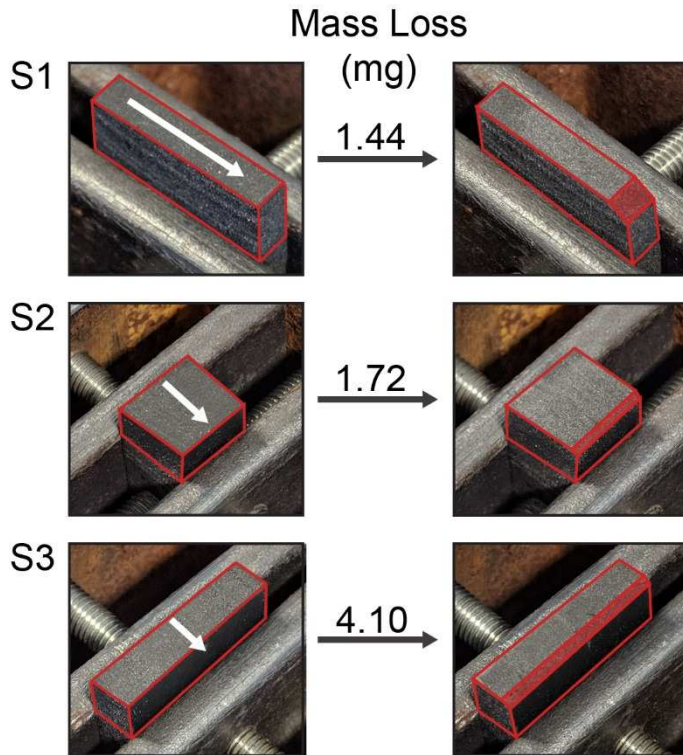


Figure 10. All three shapes before (left) and after (right) three slides at 0.2 MPa and 10 mm/s. This was done so that the wear was great enough to produce visual differences. The values for mass loss were taken from three slides at 10 N and 0.5 mm/s. The white arrows refer to the slide direction and the red lines highlight the rubber outline.

4. Discussion

The classical laws of friction say that, in dry sliding scenarios, the shape of a sliding sample has no influence on the body's friction. Figure 9 shows that this was found not to be true for the rubber tested in this study. By using rubber tread of varying second moment of area in the sliding direction and clamping them at two different heights the effect of overall beam stiffness and tread height on friction was investigated. As highlighted in Figure 8, no beam stiffness-friction relationship was found and μ_k is more affected by the sliding direction-length of the rubber (regardless of its second moment of area) and slide velocity. The effect of velocity has been well reported and as expected, the increase in velocity, in combination with the surface roughness over multiple scales, increases the oscillating frequencies transferred to the rubber. In turn, as can be observed by moving from left-to-right on the loss tangent curve of the rubber in Figure 11, the energy loss increases and therefore so does the hysteric and overall μ_k . An increase in slide velocity has been found in previous research to result in an increase in μ_k up to the velocity of around 10 mm/s where μ_k peaks [19,20]. Above this velocity, the contribution of frictional heating becomes dominate, reducing hysteresis even with the increase in oscillating frequencies [19]. Although the effect of adhesion is likely to be secondary in

comparison to hysteresis on rough surfaces, it is commonly stated that adhesion decreases with increased slide velocity beyond 10 $\mu\text{m/s}$ [21]. A combination of the frictional reductions caused by increased frictional heating and decreased adhesion is likely to explain why μ_k often peaks at 10 mm/s before dropping. However, as the maximal velocity tested here is equal to the 10 mm/s velocity threshold, the increase in velocity from 0.5 mm/s was expected to increase μ_k . Moreover, at 10 mm/s, a greater degree of stick-slip was observed which is also likely to contribute to the increased friction.

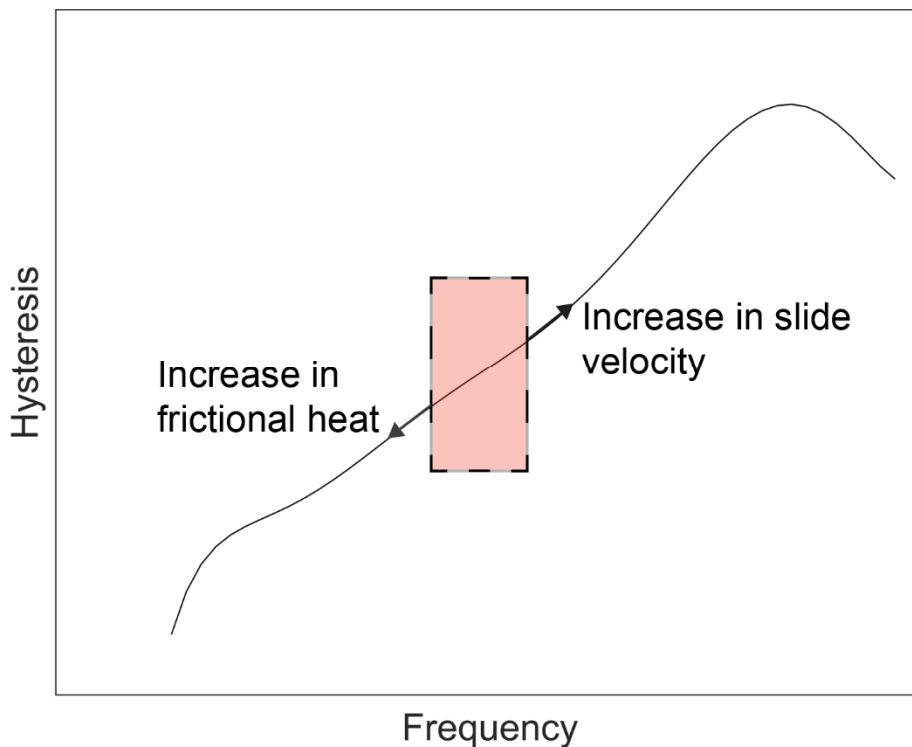


Figure 11. How the changes in μ_k recorded at different velocities can be explained through observation of the loss tangent master curve which is the ratio of real to loss modulus.

The phenomenon of shape producing different dry μ_k for rubber has been recorded in another dry rubber sliding study [1]. Fortunato et. al [1] hypothesises that the frictional difference occurs as a result of varying amounts of frictional heating, with the longer rubber shapes (parallel with the sliding direction) producing the greater amount of frictional heating. It is true that for the current study, the longer shapes produce the lowest μ_k and that this is more pronounced at the greater slide velocity at which frictional heating is likely to be influential. However, differences in μ_k were also recorded between the three rubber shapes at very slow velocities (Figure 9) at which frictional heat is unlikely to build up [1,16].

It can be suggested that there is an additional frictional mechanism that differentiates between the frictional behaviour of shapes of rubber even at velocities where frictional heat has little or no influence. By consulting the mass loss values in Figure 12, it is found that a positive correlation between wear mass and μ_k is present for the 0.5 mm/s slide velocity.

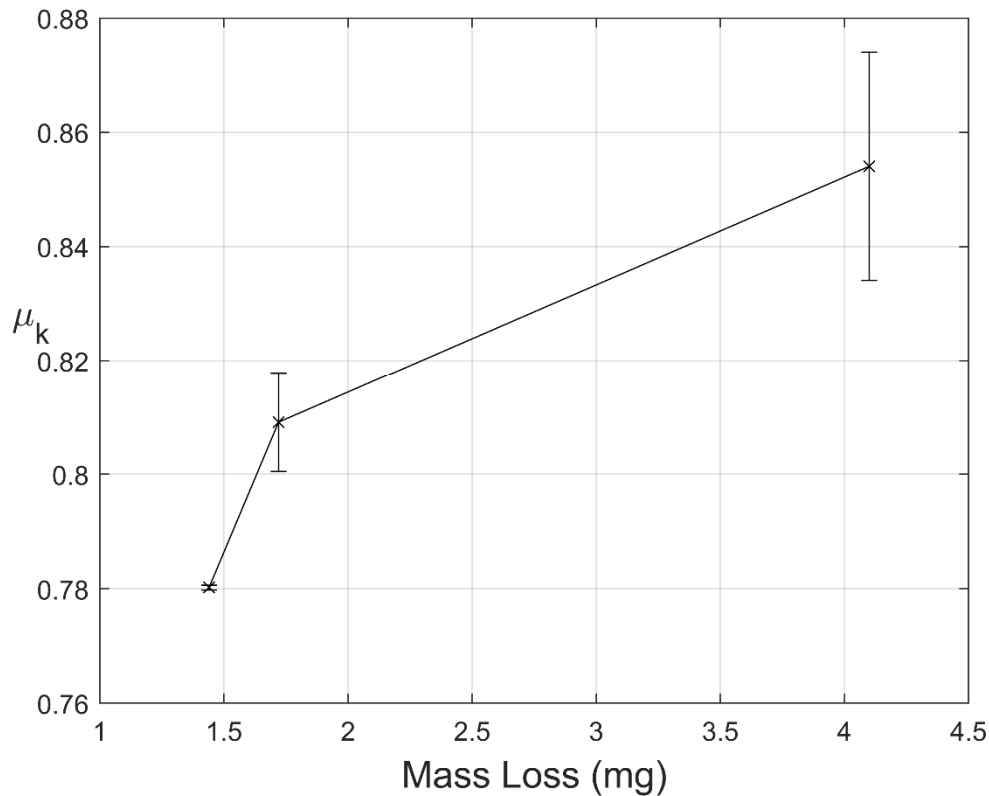


Figure 12. μ_k against mass loss for sliding at 0.5 mm/s.

The tearing of rubber by sharp surface asperities is a process which requires energy [22]. Hence, it is not surprising that the shape with the highest friction has produced the greater wear. Emami & Khaleghian [22] found the same positive correlation between mass loss and friction when sliding SBR blocks on two forms of asphalt surface. What is of interest, is why the shapes wore at different rates without the presence of frictional heating. One possible explanation is provided through interpretation of the wear images in Figure 10. The photographs show that wear mostly occurs along the leading edge of the shape. As depicted in Figure 13, Finite Element Models (FEM) such as that published by Hofstetter et al. [23] show that as rubber slides, the leading edge curls inwardly and comes under increased pressure. This is likely to increase the wear rate in that leading edge area.

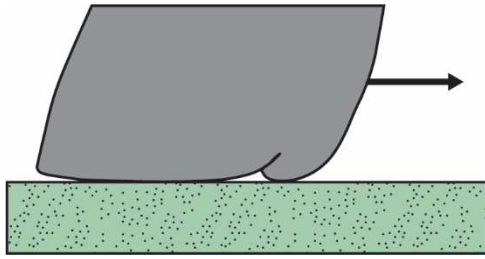


Figure 13. Depiction of leading edge effects that occur when rubber slides.

In addition to the energy consumption of the wearing process itself, this increased friction could be influenced by the changing contact area caused by wearing at this curling, leading edge. This wear gives a larger sliding contact area through chamfering. An increased sliding contact area is likely to result in increased hysteresis and adhesive energy loss which will again increase the friction.

It is theorised that in the case of this study, the increased leading edge length increases μ_k as there is a greater region of curling and therefore wearing which consumes energy. This is deemed to be the primary reason as to why shape has a frictional effect at slow velocities here. This friction mechanism will be less prominent for harder-wearing rubbers or at lower nominal contact pressures as wear is less likely to occur.

5. Conclusions

This study shows that shape has a definitive effect on the μ_k of rubber sliding over a dry rough surface. This in turn implies that different tyre and shoe treads will produce frictional differences even if the nominal contact areas are equal.

This study rejects the influence of tread beam stiffness as an influencing factor but supports the theory that, at velocities greater than 1 mm/s, longer shapes (parallel to the slide direction) have lower μ_k due to frictional heating [1]. However, as was not foreseen, a lesser but still significant frictional difference was also found at a velocity below 1 mm/s (0.5 mm/s). Investigating the wear rate and locations finds that the leading edge length also has an effect, with longer front edged shapes (perpendicular to the slide direction) producing the highest μ_k through additionally wearing.

Further studies are needed to investigate whether frictional differences in shape are noticed for slow velocities but at very low tread heights (1 – 3 mm) where leading edge curling will have less of an effect. Additionally, testing a greater variety of shapes would further indicate as to whether the observations stated here regarding a shape's slide-direction length and leading edge length, are the major frictional factors. Finally, this study only uses one grade of

rubber. Other grades of rubber may produce different frictional relationships in the conditions used in this study.

6. Acknowledgements

The authors thank Dr James Spurr and the International Tennis Federation (ITF) for their involvement and support in this research. We would also like to thank Sport Group for supplying the surfaces used.

Funding: This work was supported by the ITF and the Engineering and Physical Science Research Council (EPSRC).

7. References

- [1] Fortunato G, Ciaravola V, Furno A, Lorenz B, Persson BNJ. General theory of frictional heating with application to rubber friction. *J Phys Condens Matter* 2015. doi:10.1088/0953-8984/27/17/175008.
- [2] Persson BNJ. Theory of rubber friction and contact mechanics. *J Chem Phys* 2001. doi:10.1063/1.1388626.
- [3] Heinrich G, Klüppel M. Rubber friction, tread deformation and tire traction. *Wear* 2008. doi:10.1016/j.wear.2008.02.016.
- [4] Goff JE, Ura D, Boswell L, Carré MJ. Parametric Study of Simulated Tennis Shoe Treads. *Procedia Eng* 2016. doi:10.1016/j.proeng.2016.06.338.
- [5] Wu J, Wang YS, Su BL, Liu Q. Experimental and Numerical Studies on Tire Tread Block Friction Characteristics Based on a New Test Device. *Adv Mater Sci Eng* 2014. doi:10.1155/2014/816204.
- [6] Persson BNJ. Rubber friction: Role of the flash temperature. *J Phys Condens Matter* 2006;18:7789–823. doi:10.1088/0953-8984/18/32/025.
- [7] Kummer HW. Unified theory of rubber and tire friction. University Park : Pennsylvania State University, College of Engineering; 1966.
- [8] Maegawa S, Itoigawa F, Nakamura T. Tribology International A role of friction-induced torque in sliding friction of rubber materials. *Tribology Int* 2016;93:182–9. doi:10.1016/j.triboint.2015.08.030.
- [9] Yamaguchi T, Sugawara T, Takahashi M, Shibata K, Moriyasu K, Nishiwaki T, et al. Effect of porosity and normal load on dry sliding friction of polymer foam blocks. *Tribol Lett* 2018;66:1–9. doi:10.1007/s11249-018-0988-z.

- [10] Moriyasu K, Nishiwaki T, Shibata K, Yamaguchi T, Hokkirigawa K. Friction control of a resin foam/rubber laminated block material. *Tribol Int* 2019;136:548–55. doi:10.1016/j.triboint.2019.04.024.
- [11] Persson BNJ, Tosatti E. The effect of surface roughness on the adhesion of elastic solids. *J Chem Phys* 2001. doi:10.1063/1.1398300.
- [12] Persson BNJ, Albohr O, Tartaglino U, Volokitin AI, Tosatti E. On the nature of surface roughness with application to contact mechanics, sealing, rubber friction and adhesion. *J Phys Condens Matter* 2005. doi:10.1088/0953-8984/17/1/R01.
- [13] Ido T, Yamaguchi T, Shibata K, Matsuki K, Yumii K, Hokkirigawa K. Sliding friction characteristics of styrene butadiene rubbers with varied surface roughness under water lubrication. *Tribol Int* 2019;133:230–5. doi:10.1016/j.triboint.2019.01.015.
- [14] Scaraggi M, Persson BNJ. The effect of finite roughness size and bulk thickness on the prediction of rubber friction and contact mechanics. *Proc Inst Mech Eng Part C J Mech Eng Sci* 2016. doi:10.1177/0954406216642261.
- [15] Tiwari A, Dorogin L, Steenwyk B, Warhadpande A, Motamedi M, Fortunato G, et al. Rubber friction directional asymmetry. *Epl* 2016;116. doi:10.1209/0295-5075/116/66002.
- [16] Mahboob Kanafi M, Tuononen AJ, Dorogin L, Persson BNJ. Rubber friction on 3D-printed randomly rough surfaces at low and high sliding speeds. *Wear* 2017;376–377. doi:10.1016/j.wear.2017.01.092.
- [17] Tsai HK, Li KW, Chen CC. Effects of footwear sample area on the friction coefficient on the floor. *IEEE Int. Conf. Ind. Eng. Eng. Manag.*, 2016. doi:10.1109/IEEM.2015.7385664.
- [18] Gordon A, Glazko G, Qiu X, Yakovlev A. Control of the mean number of false discoveries, Bonferroni and stability of multiple testing. *Ann Appl Stat* 2007;1:179–90. doi:10.1214/07-aos102.
- [19] Persson BNJ. Rubber friction and tire dynamics. *J Phys Condens Matter* 2011. doi:10.1088/0953-8984/23/1/015003.
- [20] Makhovskaya Y. Modeling Sliding Friction of a Multiscale Wavy Surface over a Viscoelastic Foundation Taking into Account Adhesion. *Lubricants* 2019;7:13. doi:10.3390/lubricants7020013.
- [21] Le Gal A, Klüppel M. Investigation and modelling of rubber stationary friction on rough

surfaces. J Phys Condens Matter 2008. doi:10.1088/0953-8984/20/01/015007.

- [22] Emami A, Khaleghian S. Investigation of tribological behavior of Styrene-Butadiene Rubber compound on asphalt-like surfaces. Tribol Int 2019;136:487–95. doi:10.1016/j.triboint.2019.04.002.
- [23] Hofstetter K, Grohs C, Eberhardsteiner J, Mang HA. Sliding behaviour of simplified tire tread patterns investigated by means of FEM. Comput Struct 2006. doi:10.1016/j.compstruc.2006.01.010.